Post-breakup tectonics in southeast Brazil from thermochronological data and combined inverse-forward thermal history modeling

Nathan Cogné, Kerry Gallagher, Peter R. Cobbold, Claudio Riccomini, Cécile Gautheron

Post-breakup tectonics in southeast Brazil from thermochronological data and combined inverse-forward thermal history modeling

Nathan Cogné,[1,2] Kerry Gallagher,[1] Peter R. Cobbold,[1] Claudio Riccomini,[3] and Cecile Gautheron[4]

[1]   The continental margin of southeast Brazil is elevated. Onshore Tertiary basins and Late Cretaceous/Paleogene intrusions are good evidence for post breakup tectono-magmatic activity. To constrain the impact of post-rift reactivation on the geological history of the area, we carried out a new thermochronological study. Apatite fission track ages range from 60.7 ± 1.9 Ma to 129.3 ± 4.3 Ma, mean track lengths from 11.41 ± 0.23 μm to 14.31 ± 0.24 μm and a subset of the (U-Th)/He ages range from 45.1 ± 1.5 to 122.4 ± 2.5 Ma. Results of inverse thermal history modeling generally support the conclusions from an earlier study for a Late Cretaceous phase of cooling. Around the onshore Taubaté Basin, for a limited number of samples, the first detectable period of cooling occurred during the Early Tertiary. The inferred thermal histories for many samples also imply subsequent reheating followed by Neogene cooling. Given the uncertainty of the inversion results, we did deterministic forward modeling to assess the range of possibilities of this Tertiary part of the thermal history. The evidence for reheating seems to be robust around the Taubaté Basin, but elsewhere the data cannot discriminate between this and a less complex thermal history. However, forward modeling results and geological information support the conclusion that the whole area underwent cooling during the Neogene. The synchronicity of the cooling phases with Andean tectonics and those in NE Brazil leads us to assume a plate-wide compressional stress that reactivated inherited structures. The present-day topographic relief of the margin reflects a contribution from post-breakup reactivation and uplift.

1.   Introduction

[2]   Presently active or young rift environments tend to have elevated rift shoulders (e.g., East Africa, the Red Sea). Similarly, many older passive margins show elevated topography, with an escarpment typically occurring up to 100 km or more inland of a low-lying coastal plain [e.g., *Gilchrist and Summerfield*, 1994]. There is a continuing debate as to whether present-day high elevation is inherited from rifting or previous orogenic activity, or whether it reflects more strongly post-rift tectonic reactivation [e.g.,

Brown et al., 2002; *Cogné et al.*, 2011; *Japsen et al.*, 2012a; *Osmundsen et al.*, 2010; *Nielsen et al.*, 2009; *Persano et al.*, 2006]. The presence of such escarpments along mature passive margins today raises the question of how the relief developed over the order of 100 Ma, i.e., has any initial pre-rift or rift-related topography persisted since break-up, or has there then been some post rift uplift [e.g., *Braun and van der Beek*, 2004; *Gilchrist and Summerfield*, 1990, 1994; *Gunnell and Fleitout*, 2000; *Japsen et al.*, 2012a; *van der Beek et al.*, 1995]. To address this problem, one can consider the erosion history onshore region and use low temperature thermo-chronology, and especially apatite fission track analysis (AFT, sensitive to temperature between 120°C and 60°C) and apatite U-Th/He dating (AHe, sensitive to temperature between 80°C and 40°C) to constrain the cooling history of the upper crust (in the depth range of ∼1 to 6 km) [*Gallagher et al.*, 1998].

[3]   Some applications of such methods to passive margins led to interpretations in which rift shoulder related erosion occurred more or less continuously since rifting or even since previous orogeny [e.g., *Gallagher et al.*, 1994, 1995; *Nielsen et al.*, 2009; *Pedersen et al.*, 2012] or by discrete

[1]Geosciences Rennes, Université Rennes 1, Rennes, France.
[2]Now at Geology Department, Trinity College Dublin, Dublin, Ireland.
[3]Instituto de Geociências, Universidade de São Paulo, São Paulo, Brazil.
[4]UMR IDES, CNRS 8148, Université Paris Sud, Orsay, France.

Corresponding author: N. Cogné, Geology Department, Trinity College Dublin, Dublin 2, Ireland. (cognen@tcd.ie)
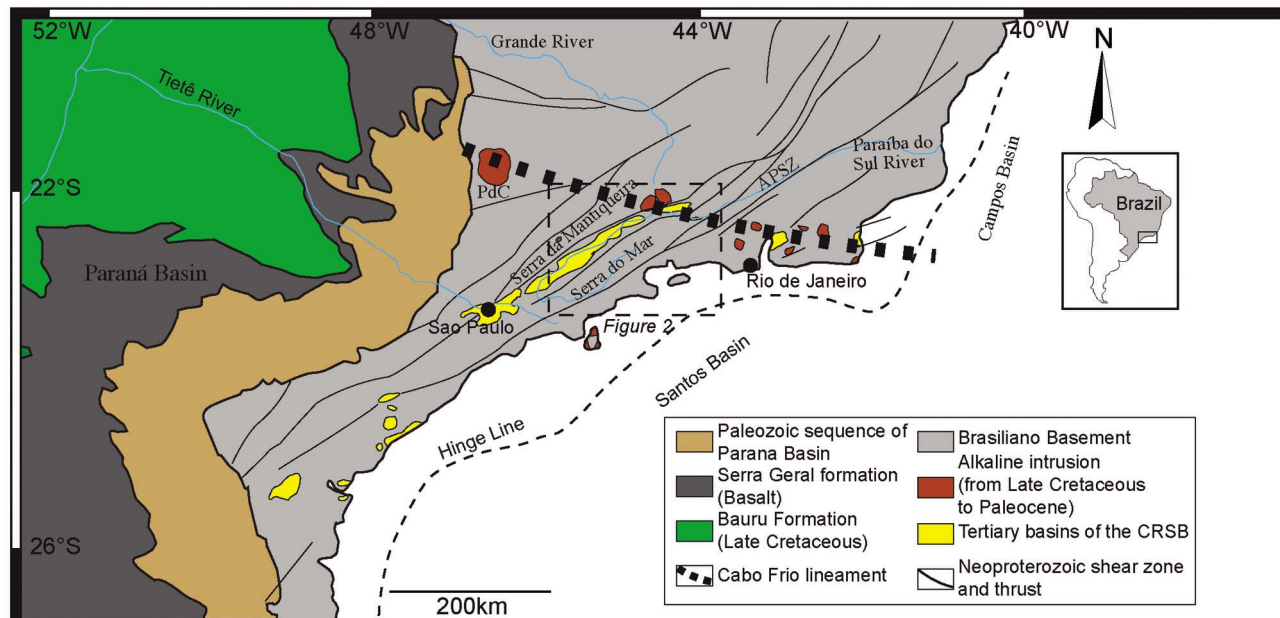
Figure 1. General map of southeast Brazilian margin showing geological framework. Dashed rectangle indicates region of Figure 2. APSZ = Além-Paraíba shear zone; Pdc = Poços de Caldas intrusion. Modified from *Hiruma et al.* [2010].

episodes linked to rifting [e.g., *Gunnell et al.*, 2003]. However, other studies inferred that the history is more complex, and that post rift events have left their mark on the thermochronological record [*Brown et al.*, 1990, 1999; *Gallagher and Brown*, 1997, 1999; *Harman et al.*, 1998, *O'Sullivan et al.*, 2000; *Raab et al.*, 2002, *Hiruma et al.*, 2010].

[4] Southeast Brazil provides a good case study area for such a debate, as it is a mature rift margin of high relief, which formed during rifting of the South Atlantic around 130 Ma [*Chang et al.*, 1992; *Nürnberg and Müller*, 1991]. The onshore margin exhibits good evidence for post-rift reactivation of the Precambrian basement, in terms of (1) a series of Late Cretaceous to Palaeocene alkaline plutonic bodies and (2) a series of onshore Tertiary basins that lie in the Paraiba do Sul valley (Figure 1). Such evidence for post-breakup tectonic activity raises the possibility of assessing the impact of such activity on the present-day landscape.

[5] In this contribution we present new thermochronological data from southeast Brazil and more specifically from the Taubaté and Resende Tertiary basins, the adjacent areas of high relief (i.e., Serra da Mantiqueira and Serra do Mar) and the Atlantic coast (Figure 2), with the aim of better constraining the Tertiary cooling history and tectonic activity. After a brief review of the geological setting and the AFT and AHe methodologies, we describe the data and our modeling approaches. We then discuss our results qualitatively and quantitatively and integrate them with available geological data to constrain the post-rift evolution of the margin and to assess the possible causes of post-rift reactivation.

2. Geological Setting

[6] Here, we only briefly describe the main geological features of the SE Brazilian margin, but for more details,

see *Cogné et al.* [2011]. Onshore, the outcrop is mainly Precambrian basement, which formed during the Brasiliano orogeny (700 to 450 Ma) [*de Brito-Neves and Cordani*, 1991; *Trouw et al.*, 2000] and is cut by major shear zones (trending NE-SW) and thrusts (trending N-S). Alkaline bodies intruded this basement during the Late Cretaceous and Palaeocene, mainly along the Cabo Frio lineament [*Almeida*, 1991, Figure 1]. In our studied area, Tertiary basins, with a thickness of sediments that can reach 800 m [e.g., *Riccomini et al.*, 2004] lie in the Paraiba do Sul valley. According to some authors [e.g., *Almeida*, 1976; *Riccomini et al.*, 2004], these basins formed by rifting, whereas others [e.g., *Cobbold et al.*, 2001; *Cogné et al.*, 2012; *Padilha et al.*, 1991] have favored a transtensional (pull-apart) context. The basins are at least 48 ± 1 Ma old (from ^{40}Ar-^{39}Ar dating of intercalated lavas in the Volta Redonda Basin [*Riccomini et al.*, 2004]), but could be as old as Palaeocene [*Cobbold et al.*, 2001; *Cogné et al.*, 2012; *Sant'Anna et al.*, 2004].

[7] The main topographic features onshore, between São Paulo and Rio de Janeiro, are, from SE to NW, (1) a low coastal plain, (2) a scarp (1000 to 1500 m) leading to the Serra do Mar, (3) the plateau of the Paraiba do Sul valley (400 m to 600 m), (4) a second scarp, at the southeastern edge of the Serra da Mantiqueira (~2000 m with summit that reach 2800 m) and (5) a hinterland plateau (Figures 2 and 3).

[8] Offshore, seismic and stratigraphic studies for petroleum exploration have led to a good understanding of the structure of the Santos Basin [e.g., *Contreras et al.*, 2010; *Leyden et al.*, 1971; *Modica and Brush*, 2004; *Pereira and Macedo*, 1990] and Campos Basin [e.g., *Contreras et al.*, 2010; *Mohriak et al.*, 1990, 2008]. These studies show that the basins are mostly typical of a passive
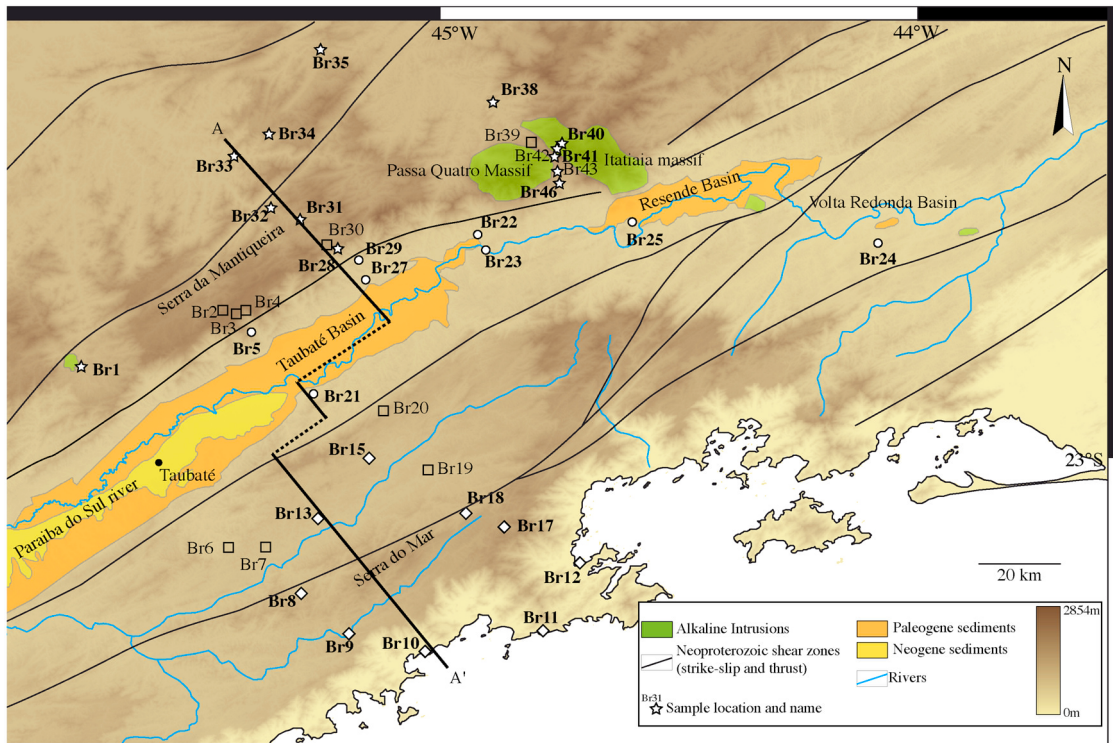
Figure 2. Simplified geological map of study area (for location, see Figure 1). All outcrops are of Precambrian basement, except in colored areas. Samples are from three areas, Serra da Mantiqueira (white stars), Tertiary basins (white circles) and Serra do Mar – coastal area (white diamonds). Samples without AHe or AFT data (open squares) we have not used for interpretations. Topography is from Shuttle Radar Topography Mission (SRTM), 3 arc-second. For topographic profile A-A′, see Figures 3 and 10.

margin, but underwent tectonic reactivation during the Late Cretaceous and Palaeogene for the Santos Basin [*Cobbold et al.*, 2001], as well as the Neogene for the Campos Basin [*Cobbold et al.*, 2001; *Fetter*, 2009]. Moreover the spatial distribution of sediment indicates a highly variable flux over time, potentially due to variations in the rate of onshore erosion, or to changing source

regions [e.g., *Cobbold et al.*, 2001; *Contreras et al.*, 2010; *Mohriak et al.*, 2008].

3. Sampling Strategy for Low Temperature Thermochronology

[9] Previous thermochronological studies (mainly using only AFT) have led to interpretations in terms of both
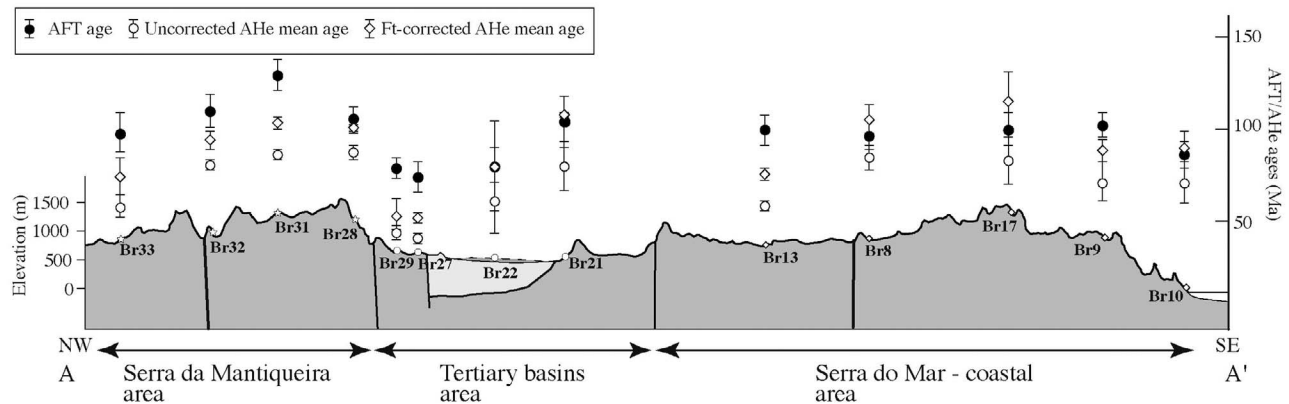

Figure 3. Representative topographic cross-section of study area (see Figure 2 for line of profile), together with AFT ages, uncorrected AHe ages and F_T corrected AHe ages of samples from three areas (as in Figure 2).

continuous and episodic denudation [*Gallagher et al.*, 1994, 1995; *Hiruma et al.*, 2010; *Tello-Saenz et al.*, 2003, 2005]. Many of the AFT-inferred local denudation rates have Upper Cretaceous to Cenozoic peaks [*Hackspacher et al.*, 2008; *Hiruma et al.*, 2010; *Tello-Saenz et al.*, 2003, 2005], i.e., post-break-up. In a recent study, *Cogné et al.* [2011] presented a suite of new U-Th/He data on samples (mainly from Precambrian basement but also from the Poços de Caldas intrusion) previously used for AFT by *Gallagher et al.* [1994]. The results were similar to those of *Ribeiro* [2007] from a more restricted area, in implying widespread cooling during the Late Cretaceous. However, due to the relatively low temperatures (around surface temperature, i.e., 20–30°C) after Late Cretaceous cooling, the constraints on the Tertiary history were quite equivocal. Only 2 samples suggested a discrete cooling phase in the Neogene while others implied protracted cooling or near-surface temperatures during all of the Tertiary.

[10] We collected 45 new samples from (1) Precambrian basement rocks around the Taubaté Basin, (2) the adjacent Serra do Mar and Serra da Mantequeira (including two samples in the Itatiaia massif) and (3) the coastal region. We focused specifically on the area where we considered there to be the best opportunities to identify Late Cretaceous to Tertiary tectonic activity onshore given the presence of Tertiary basins. For each sample we separated apatite from around 5 kg of rock, by traditional magnetic and heavy liquid methods. Of the samples, 39 yielded apatite, but only 35 had enough for both fission track and (U-Th)/He analyses.

4. Thermochronology

4.1. Apatite Fission Track Analysis

[11] We use the external detector method [*Gleadow*, 1981; *Hurford and Green*, 1982]. The apatite separates were embedded in epoxy resin, polished to expose an internal surface, and the spontaneous tracks are revealed by 6.5% HNO_3 during 45 s at 20°C. Afterwards we attached a low-U external mica sheet and all samples were irradiated in the Oregon State University Radiation Center together with CN5 dosimeters. The induced tracks in the mica were etched with 60% HF for 40 min at 20°C. NC did all the AFT measurements in Rennes with a Zeiss M1 microscope with dry magnification of ×1000, using Trackscan® software. For each sample we counted a minimum of 20 single grains using the ζ calibration method [*Hurford and Green*, 1983; *Hurford*, 1990] with a ζ value equal to 316.70 ± 3.03 a.cm². The central age [*Galbraith and Laslett*, 1993], radial plot [*Galbraith*, 1990], and single grain age distribution were calculated with Trackkey software [*Dunkl*, 2002]. When it was possible we measured 100 horizontal confined tracks for the length distribution [*Gallagher et al.*, 1998; *Gleadow et al.*, 1986] and their orientation to c-axis, as both the annealing and etching of tracks are anisotropic [*Barbarand et al.*, 2003a; *Donelick*, 1991; *Ketcham et al.*, 2007]. We also measured the long axis of the etch pits, Dpar, as a proxy for the compositional dependence of annealing [*Barbarand et al.*, 2003b; *Carlson et al.*, 1999; *Ketcham et al.*, 2007].

4.2. (U-Th)/He Analysis

[12] He in apatite is quantitatively retained at temperatures below 40°C and the system is typically considered open at temperatures above 80–90°C [*Farley*, 2000; *Wolf et al.*, 1996, 1998], defining the He partial retention zone (HePRZ). The effective closure temperature varies with cooling rate and composition [*Warnock et al.*, 1997] and with crystal size [*Farley*, 2000; *Reiners and Farley*, 2001] but has been reported for Durango apatite around 65 ± 10°C [e.g., *Cherniak et al.*, 2009; *Ehlers and Farley*, 2003; *Farley*, 2000].

[13] The diffusive loss of He is also a function of radiation damage, produced by α-recoil, leading to enhanced He retention for apatites with higher U and Th concentrations [*Flowers et al.*, 2009; *Gautheron et al.*, 2009; *Shuster et al.*, 2006; *Shuster and Farley*, 2009]. Additionally, α-ejection can lead to non-diffusive He loss within about 20 μm of the crystal edge. To account for this, the measured age can be corrected by an F_T factor, which is a function of the surface/volume ratio of the crystal grain [*Farley et al.*, 1996; *Gautheron et al.*, 2006]. Alternatively, the α-ejection process can be allowed for explicitly during thermal modeling [*Meesters and Dunai*, 2002]. Here, the AHe ages are corrected for alpha ejection using the F_T ejection factor, because it can lead to a more representative age for comparison with the AFT ages [see *Gautheron et al.*, 2012]. However, the He concentration profile close to the boundary of a crystal reflects both the ejection factor and thermally induced diffusion. As the rate of diffusion is also controlled by the concentration gradient at the boundary we use the uncorrected age when modeling the thermal history, and apply the α-ejection correction at each model time step (as suggested by *Meesters and Dunai* [2002]).

[14] Apatites were selected (by NC) under an Olympus SZX2–16 microscope at a magnification of ×120, according to their shape, size, and lack of obvious fractures or U-Th-rich inclusions. The selected crystals were grouped into 3–5 separate aliquots (containing 1, or rarely 2 similar crystals) for each sample, put into a Pt tube and heated by laser to degas He at temperatures around 1000°C. The amount of He was measured by a quadrupole mass spectrometer. Reheating was undertaken to test the total degassing and the possible presence of unidentified U-Th rich inclusions during picking. Following *Farley* [2002], an aliquot was rejected if the re-extract was greater than the blank value at more than 1.5%. After degassing, we used isotopic dilution by spiking the samples with a known amount of ^{235}U and ^{230}Th and measured the amounts of ^{238}U and ^{232}Th by ICP-MS.

[15] Some of the analyses were done at the Scottish Universities Environmental Research Centre (SUERC), and the remainder at the Interactions et Dynamiques des Environnements de Surface (IDES) laboratory at Orsay University. Errors on AHe age should be considered as up to about 8% corresponding to the dispersion of measured standards.

5. Results

5.1. Apatite Fission Tracks Data

[16] The AFT ages range from 60.7 ± 1.9 to 129.3 ± 4.3 Ma (Figure 4) and the mean track length ranges from 11.41 ± 0.23 μm to 14.31 ± 0.24 μm (after c-axis correction), the standard deviation being between 1.01 μm and 2.46 μm (see auxiliary material).[1] Dpar values range

---

[1]Auxiliary materials are available in the HTML. doi:10.1029/2012JB009340.
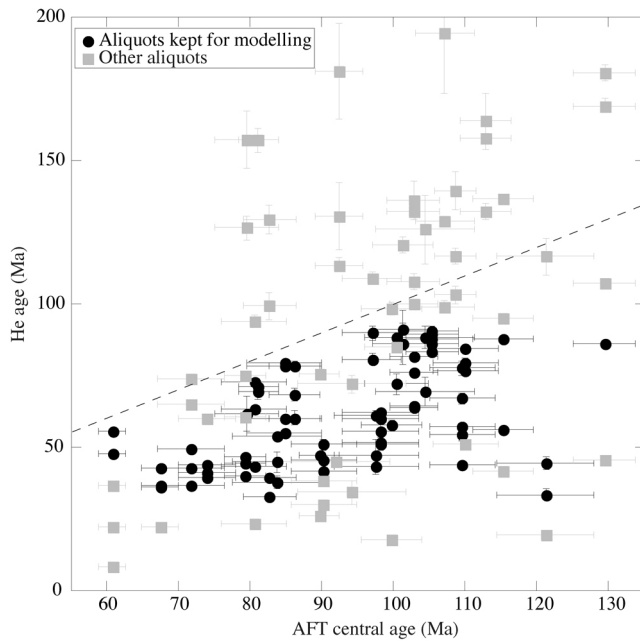
Figure 4. Plot of individual AHe ages versus AFT central ages, showing aliquots that we kept for modeling and those that we rejected.

from 1.3 to 1.8 μm, indicating F-apatites that are less resistant to annealing than Durango (mean Dpar of 1.91 μm with same condition of annealing).

[17] The single grain ages show no statistically significant dispersion, all the samples passed the χ^2 test and the single grain age distributions were unimodal. On an AFT age vs mean track length plot, the mean track length decreases slightly with age, but do not display the boomerang form [*Gallagher and Brown*, 1997; *Green*, 1986], characteristic of a rapid cooling from different initial temperatures. As the oldest age is about equal to the time of rifting, this "lack of boomerang" indicates a more complex history since rifting. There is no obvious relation between age and distance to the coast, while the ages show a tendency to increase with altitude (except for the 2 samples from the Itatiaia pluton, Figure 2).

5.2. AHe Age Data

[18] Uncorrected single grain AHe ages (with measured error) range from 8.6 ± 0.1 to 393.5 ± 12.6 Ma with corresponding F_T-corrected ages of 10.1 ± 0.1 to 519.6 ± 16.6 Ma. We often obtained large ranges in AHe age with aliquots from the same sample (dispersion can be more than 100%). There are various explanations for the variation in AHe ages between and within samples [see *Cogné et al.*, 2011; *Fitzgerald et al.*, 2006] and we detail below how we consider the AHe ages, so as to assess their consistency and then select a subset of the data. The AHe data that we selected in this way (see auxiliary material) have ages ranging from 33.0 ± 1.1 Ma to 90.9 ± 7.0 Ma (uncorrected, Figure 4) and from 45.1 ± 1.5 to 122.4 ± 2.5 Ma (F_T-corrected). All the selected uncorrected ages are younger than the corresponding AFT age, and while some corrected ages are slightly older, they are consistent at the 2σ error level. The AHe ages increase slightly with altitude

(Figure 3), while there is no obvious correlation with distance to the coast. All the selected AHe ages are younger than rifting and some of them are Tertiary, implying cooling and perhaps tectonic activity during this period.

6. Interpretation

[19] For a given thermal history, we use the annealing models of *Ketcham et al.* [2007] to simulate AFT data and a standard spherical diffusion model combined with the radiation damage model of *Gautheron et al.* [2009] for AHe ages. Using the inversion approach described in *Gallagher* [2012] we sample many different thermal histories and construct a population of models, by either retaining or rejecting different models probabilistically, based on the fit to the observations. In this section, we first describe how, for a given sample, we use an iterative inversion-based approach to assess the internal consistency of the observed AHe ages and also their consistency with both AFT and geological data. Subsequently, we use forward modeling with specific thermal histories. The aim is to assess the resolution of variability in the post-rift part of the thermal histories, given the uncertainty range inferred for the inverse models.

6.1. Assessing the AHe Age Data

[20] There is a range of explanations for AHe age dispersion within and between samples, that has been previously observed in cratonic areas, for example. These include unrecognized U-Th rich inclusions, U-Th zonation, grain size variations or enhanced He retention by radiation damage (for a more detailed review of these factors see *Fitzgerald et al.* [2006] and *Cogné et al.* [2011]). However, as described in *Cogné et al.* [2011], the observed dispersion in our AHe data cannot be fully explained by these factors. Recently, *Brown et al.* [2011] have shown that analyzing broken crystals can lead to a large spread in single grain AHe ages. Synthetic models suggest that the true age is around the mean age, and therefore it may be justifiable to effectively reject the oldest and youngest ages and to consider those closer to the mean. Similarly, *Flowers and Kelley* [2011] suggest that it is valid to reject some of the data if it is not possible to reconcile the observed range of different AHe ages. In assessing the fidelity of the data, we proceed as follows:

[21] (1) First we exclude samples for which we do not have AFT data as a cross-check on the AHe ages, because generally AHe age data alone cannot yield particularly well-constrained temperature history models.

[22] (2) Second, we exclude all the AHe ages that are older than corresponding AFT ages, if grain size or effective uranium (eU) concentration cannot explain the differences.

[23] (3) Subsequently we ran the inverse modeling with all the remaining AHe age data and AFT data for each sample, and then examined the fit between each predicted and observed AHe age to assess their internal consistency and also their consistency with the AFT data.

[24] (4) In the situation where one AHe age was distinctly different from others (and the variations were not correlated with size or eU), and this age was consistently badly predicted, we excluded it.

[25] (5) Another situation arose when we had two distinct groups of predictions. In this case different constraints were

applied to try to identify the more acceptable of the two possibilities. First we ran separately the two configurations with the AFT data and examined how the predictions fit both the AFT and AHe data together. Usually one possibility gave significantly better predictions than the others. Second, we considered the consistency of the AHe data with nearby samples if no major faults had been reported between them.

[26] As a consequence of this procedure we excluded the samples Br4, Br20, Br30, Br39, Br42 (no or too few AFT data) from the subsequent interpretations. Neither Br6 nor Br43 with He data give temperature history with good predictions whatever the configuration of single aliquot ages considered. After this selection process, we ended up with 6 samples with AFT data (ages, track length distribution) only and 28 samples with AFT data and between 1 and 5 aliquots of AHe ages. From these 28 samples about a third of the AHe data have been culled of (Figure 4). This is an important proportion and for some samples the majority of AHe data have been rejected. However, inclusion of these rejected samples does not change the overall interpretations as the other more coherent data (and the AFT data) have a greater influence in determining the thermal history solutions. Therefore, we believe this modeling based selection makes the use of the AHe data more robust and reliable for constraining the thermal history. Samples with only AFT data provide fewer constraints on the thermal history, often leading to just protracted cooling histories with no structure in the Tertiary (see *Cogné et al.* [2011] for comparison between modeling with AFT and AHe data and with AFT data only). Therefore these samples are less informative, so we do not consider them for the main interpretations.

6.2. Results of Inverse Modeling

[27] Thermal histories for expected and maximum likelihood models with predictions are show in Figure 5 for 4 samples (Br9, Br22, Br28, Br29) that we consider are representative, in term of ages data and modeling results, of the evolution of the area. The detailed results for all samples are available in the auxiliary material while the mean or expected thermal history models [see *Gallagher*, 2012] using both AFT and AHe data are summarized in Figure 6.

[28] In the Serra do Mar and coastal area (Figure 2, 3, and 6a) we infer a period of rapid cooling during the Late Cretaceous between 100 Ma and 70 Ma. The amount of cooling is about 50°C at a mean rate of 2.5°C/m.y. or so. Following this cooling samples underwent an apparent reheating of between 10 and 25°C until Neogene. From 15 Ma, we identified a second phase of accelerated cooling (2.5°C/m.y) until the present-day.

[29] In the Serra da Mantiqueira area (Figure 2, 3, and 6b) we identified the same Late Cretaceous phase of cooling as inferred for the Serra do Mar. This cooling range from 65 to 35°C at rates between 2 to 4.5°C/m.y. Br40 and Br41, from the Late Cretaceous Itatiaia intrusion, show rapid cooling after the emplacement of the intrusive body and then a monotonic cooling until present-day. Similar to the Serra do Mar, most of the samples underwent an apparent reheating of about 20°C after the Cretaceous cooling before a period of accelerated cooling from 15 Ma. The amount and rate of the inferred Neogene cooling are similar to these of the Serra do Mar. We return to the significance of this later.

[30] Between the two Serra lie the Tertiary basins (Figure 2, 3, and 6c). Here two samples, Br22 and Br25 also imply Late Cretaceous cooling of about 30°C at a rate of 1.3°C/m.y. On the southeastern border of the Taubaté basin, Br21 appears to have begun cooling earlier and more rapidly at about 3°C/m.y. On the northwestern border, two samples, Br27 and Br29 suggest cooling of 55–60°C during the Eocene at a rate of 3.5–4.0°C/m.y., while a third one, Br5, started to cool earlier during the Palaeocene. For some samples close to the basin margins (Br21, Br27 and Br29 and to a lesser extent Br25), the initial period of cooling is followed by an apparent reheating of about 20°C. Finally in this area the model results also imply a period of rapid cooling during the Neogene, similar to that inferred for the two Serras.

[31] Overall, only few samples imply cooling around the timing of rifting (∼130 Ma). This is consistent with the conclusions of *Cogné et al.* [2011], where only one sample showed cooling at this time. This may simply be a reflection of the samples remaining above the Partial Annealing Zone (PAZ) after rifting rather than there being no thermal effect. We infer 3 subsequent phases of post-rift cooling. The first during Late Cretaceous affects the whole area. The second during Palaeocene and Eocene is only resolved on the northwest border of the Taubaté basin. Finally the whole area also seems to have experienced a cooling since ∼15 Ma, i.e., Neogene. Most of the samples also have an apparent reheating between the two.

[32] With the Bayesian approach we adopt for the inverse modeling, the probability distribution on temperature (at a given time) and associated 95% credible intervals are an indication of the uncertainty on the inferred temperature history. For the Tertiary we have 20 samples that show a Neogene cooling phase of magnitude that range between 40 to 20°C. Of those samples, a large number also imply a reheating phase from surface temperatures before this last cooling. However, the reheating and the cooling are in a temperature range near the resolution limits of the thermochronological methods (i.e., temperatures <50–60°C) and the 95% credible intervals leave a range of possibilities for thermal history.

6.3. Forward Modeling

[33] Following from the inverse modeling and the fact that the thermal histories have uncertainties, we want to test different thermal histories scenarios consistent with these uncertainties. We stress here that these model results are always conditional on the assumed kinetics for fission track annealing and AHe diffusion. Therefore, while we consider the range of predictions for the different forward models considered, we are not testing the validity of the annealing or diffusion models.

[34] We start with a representative thermal history model obtained from the expected model of inverse modeling (depicted in Figures 7 and 8 by model E). In general, this has an initial cooling episode, followed by either reheating or a period where the temperature remains more or less constant, with a final period of cooling in the late Tertiary. Given such a reference model, we then consider the following variations:

[35] (1) The first cooling phase, before the reheating, does not cool to surface temperatures but remain at a relatively
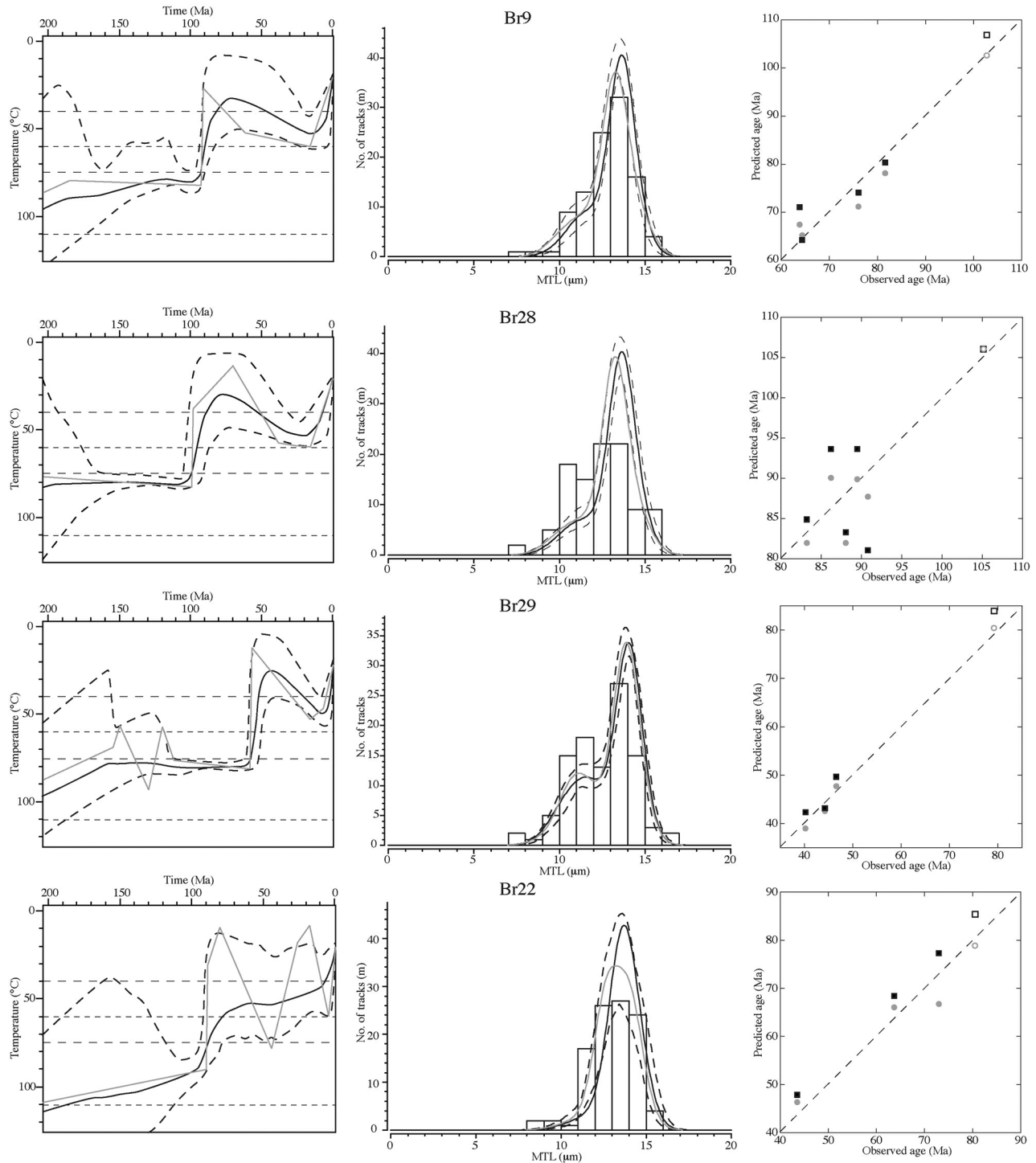
Figure 5. Results of inverse modeling for 4 representative samples. For each sample, graph on left shows inferred thermal history models. Solid black line is expected model with 95% credible interval range (dashed lines); solid gray line is maximum likelihood (best data fitting) model. Thin dashed black lines approximate AFT PAZ (short dash) and AHe PRZ (long dash) and PRZ is for standard (Durango) kinetics. Graphs in center show predicted and observed (histogram) track length distributions, for expected model in black line, with 95% credible interval range on predictions in dashed black, and for maximum likelihood model in gray line. Graphs on right are predictions of ages as functions of observed (measured) ages, black squares are for expected model, gray circles are for maximum likelihood model, filled symbols are for AHe and open symbols are for AFT. Dashed line is 1:1 line.
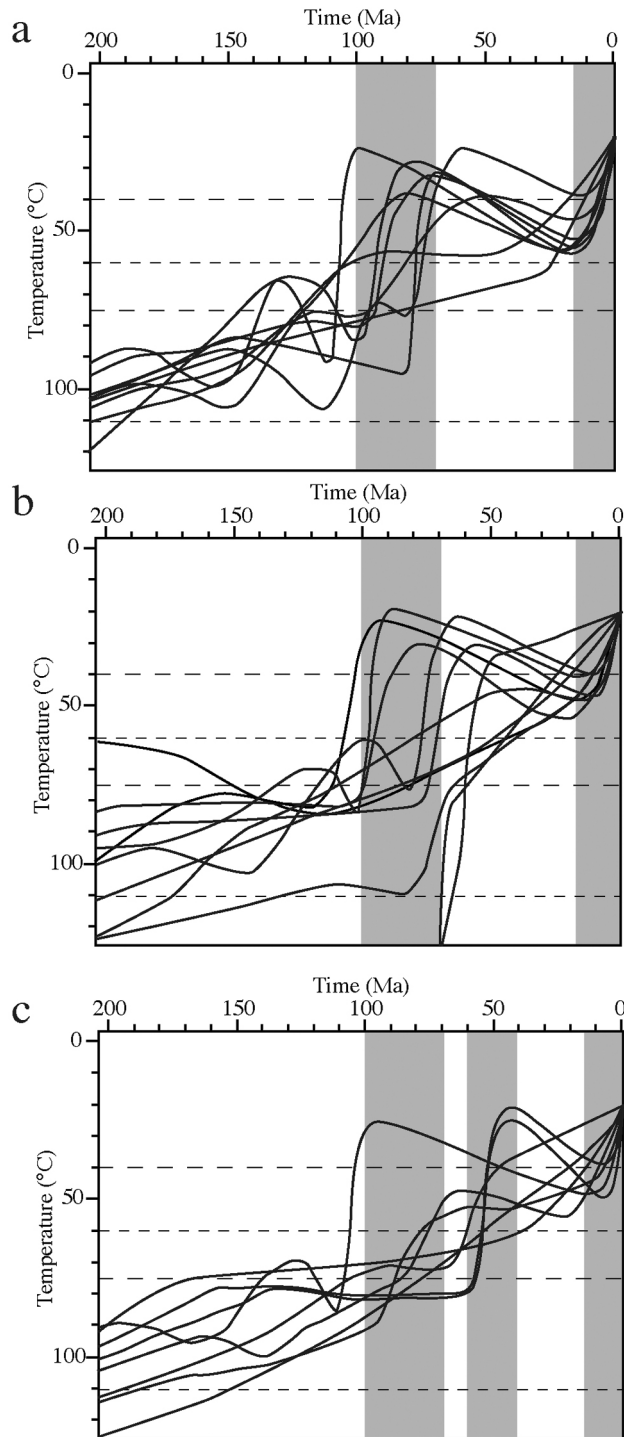
Figure 6. Post 200 Ma inferred thermal histories for expected models for samples with both (U-Th)/He and AFT ages. Grey bars represent periods of post-breakup cooling, inferred from inverse modeling, for (a) Serra do Mar and Coastal area (Br6 to Br18), (b) Serra de Mantiqueira (Br1, Br28 and Br31 to Br46) and (c) area of Tertiary basins (Br5, Br21 to Br27 and Br29). Thin dashed black lines are for AFT PAZ and AHe PRZ. PRZ is for standard Durango kinetics.

high and constant temperature during the Palaeogene and then cools during the Neogene (prolonged heating, depicted by model 1 in Figures 7 and 8).

[36] (2) The sample experienced cooling to the surface and then remains at the surface until present-day (no reheating, depicted by model 2 in Figures 7 and 8).

[37] (3) The first cooling phase does not cool to surface temperatures. Then the sample experiences a protracted second cooling to the present-day temperature (protracted cooling, depicted by model 3 in Figures 7 and 8).

[38] (4) For samples that do not show reheating after the first cooling, we force a reheating before the final cooling in Neogene (forced reheating, depicted by model 4 in Figure 8).

[39] In Figure 7 we show the different thermal histories modeled and the predictions for 2 representative samples, in terms of data and modeling results, Br 9 for the Serra do Mar and Br28 for the Serra da Mantiqueira. If temperature stays below ~50–55°C, the AHe data cannot readily discriminate between the different predictions as they are more or less all the same. The AFT data and especially track length distribution do imply a cooling event during the Neogene with or without a previous reheating. If we do not include this Neogene cooling, the predicted tracks lengths are too long. Finally there is no notable difference in the predictions for a thermal history with reheating during Palaeogene and a Neogene cooling or a constant Palaeogene temperature and then a Neogene cooling.

[40] The forward model results for two samples (Br27 and Br29) show a different pattern to those discussed above (see Figure 8a for Br29). For these samples the most consistent solution is early Tertiary cooling followed by reheating and Neogene cooling as given by inverse modeling (see Figure 5 for Br29, and auxiliary material for Br27). In the case of a Tertiary history resting at surface temperatures, the AFT predictions are poor relative to the observed values, whereas if the samples stay at higher temperatures (40–50°C), the predicted AHe ages are too young. For these two samples, a reheating after the first cooling phase, following by another recent cooling, are required to explain the observed AFT and AHe data properly. These samples are from the northern border of the Taubaté basin, between the sediments and the Sierra da Mantequiera.

[41] Five other samples (Br5, Br21, Br22, Br23, Br25) are also located near the boundaries of the Taubaté-Resende basins. From the inverse modeling stage, only the expected model for Br21 implies reheating. However, the expected models for these samples (except Br23) show a Late Cretaceous and/or Palaeogene cooling. We then examined these inferences with forward models that involve reheating following this cooling phase. The results for these tests show that the data allow a reheating phase similar to samples Br27 and Br29, and once again this is compatible with uncertainties on the thermal histories obtained from the inverse modeling (for example see model 4 in Figure 8b for Br22).

[42] Therefore we conclude that, conditional on the assumed kinetic models for AFT annealing and AHe diffusion, for the samples of the Serra do Mar and Serra da Mantiqueira, the Palaeogene reheating is not really required, because we can obtain similar predictions without it. However, the Neogene cooling is required to explain data adequately. In contrast some samples (Br27 and Br29) from
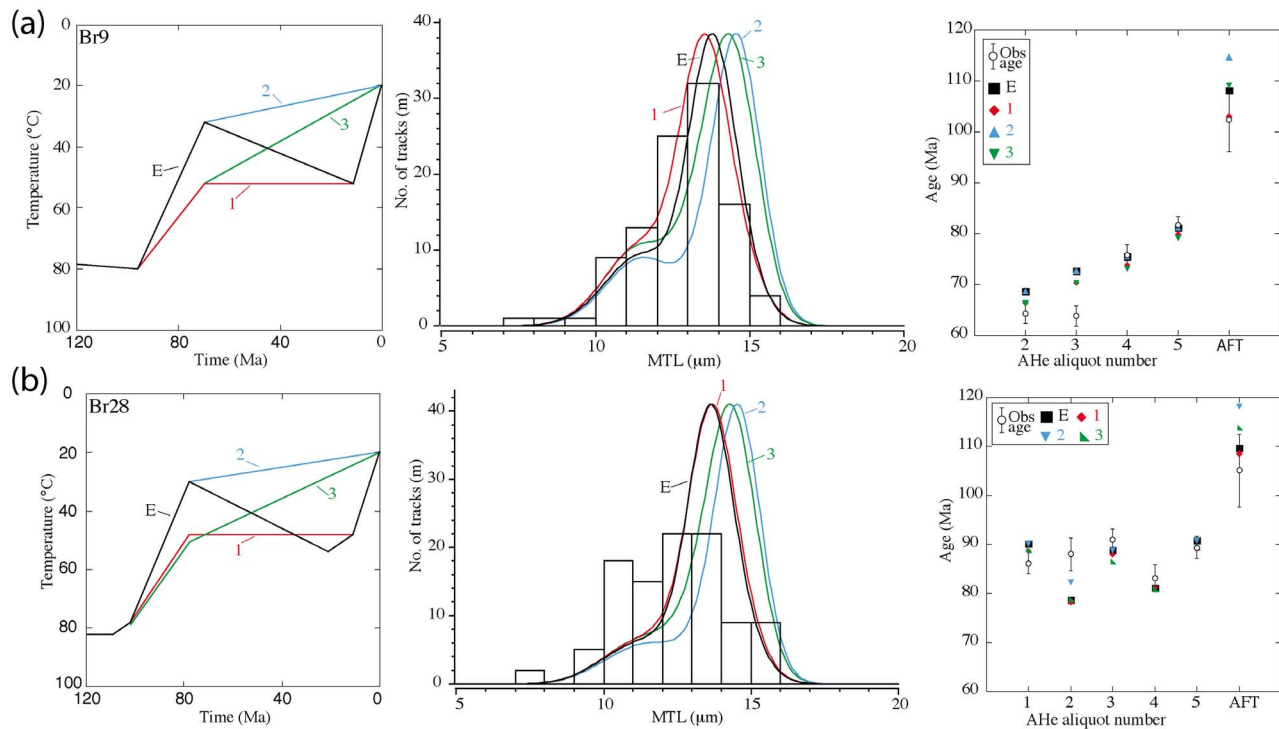
Figure 7. Forward modeling results for 2 samples representative of (a) Serra do Mar (Br9) and (b) Serra da Mantiqueira (Br28). For each sample, graph on left is for thermal histories that we have considered (we show here only that part of thermal history that we changed for the different models, for the older part of thermal histories please refer to Figure 5). E is expected model from inverse modeling, 1 is for prolonged heating, 2 is without reheating, 3 is with protracted cooling. Graphs in center summarize predictions of track length distribution for each thermal history (E, 1, 2 and 3, as in left graphs). Graphs on right show AHe and AFT age predictions for each thermal history. Observations are in open symbols, predictions in filled symbols (E, 1, 2 and 3 as in left graphs). Overall data do not require reheating but do require Neogene cooling to be predicted adequately.

around the margins of the Tertiary basins area require a reheating to fit the data as well as a Neogene cooling. For the others samples of the Tertiary basin area the forward model results show that model predictions are similar with a reheating and without. Thus there appears to be a difference between the thermal histories experienced by samples on the Serras and the samples of the Paraiba do Sul valley.

7. Discussion

7.1. Episodes of Post-Rift Cooling

[43] The lack of correlation between AFT and AHe ages and the distance to the coast implies that the development of the Serras in SE Brazil is not simply due to scarp retreat of the initial rift shoulder. In contrast, given the range of thermal histories from inverse and forward modeling of the new AFT and AHe data, we infer up to 3 periods of post-rift rapid cooling (Figures 6 and 9). Over the whole area two periods seem important, one during the Late Cretaceous and the other during the Neogene. On the northwest border of the Taubaté Basin, the 3 samples between the basin and the scarp of the Serra da Mantiqueira (Br5, Br27 and Br29) show Early Tertiary cooling of a magnitude equivalent to that experienced during the Late Cretaceous for the other samples. The thermal histories of these 3 samples do not

show Late Cretaceous cooling, probably because subsequent cooling dominates the data record. Because of the results of the sensitivity tests with forward modeling, conditional on the assumed kinetic model, we also infer that the reheating after the first period of cooling is not well constrained by data for the Serra do Mar and Serra da Mantiqueira. However, in the area of Tertiary basins the data for samples that show such reheating require it. To summarize the outcome of this combined modeling process, we present representative thermal histories in Figure 9.

7.2. Late Cretaceous Cooling

[44] The samples imply a first post-rift phase of cooling between 100 Ma and 70 Ma over the whole study area (Figures 9 and 10), consistent with the conclusions of *Cogné et al.* [2011]. In NE Brazil, *Harman et al.* [1998] inferred a similar timing of cooling around the E-W Pernambuco shear zone. *Japsen et al.* [2012b] and *Cobbold et al.* [2010], also report an exhumation phase during the Campanian in NE Brazil, of comparable magnitude to ours. There is also a tectonic reactivation during the Campanian in the Santos basin, offshore of our studied area, where the whole Cretaceous sequence tilted by up to 20° [*Cobbold et al.*, 2001; *Contreras et al.*, 2010; *Zalan and de Oliveira*, 2005]. As the proximal deposits are coarse-grained and the rate of
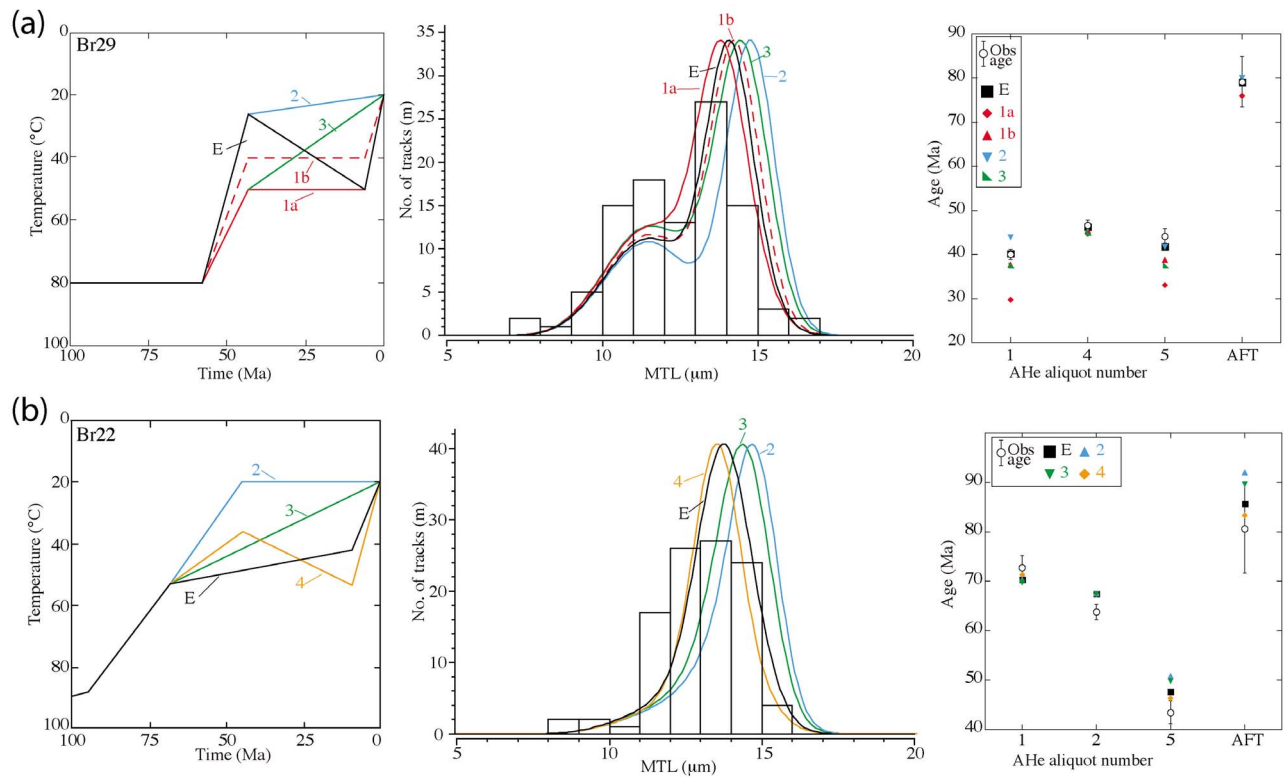
Figure 8. Forward modeling results for 2 samples representative of Tertiary basins, (a) one with inverse modeled thermal history (Br29) showing reheating and (b) the other without such reheating (Br22). Models E, 1, 2 and 3 are the same than in Figure 7, model 4 is for forced reheating. Please note that for Br22 there is no model 1 given that expected model already shows a prolonged heating. Overall data for Br29 require a period of reheating and Neogene cooling for proper predictions, whereas predictions for Br22 appear to be more consistent with observed data if there is a reheating.

deposition was higher than in other periods, several authors have argued for uplift of the coastal range [e.g., *Almeida and Carneiro*, 1998; *Assine et al.*, 2008; *Bacoccoli and Aranha*, 1984; *Cobbold et al.*, 2001; *Modica and Brush*, 2004; *Mohriak et al.*, 2008]. Onshore, alkaline bodies intruded Precambrian basement during the Late Cretaceous and Early Tertiary. These intrusions lie along a major transfer zone between the Santos and Campos basins, so *Cobbold et al.* [2001] and *Riccomini et al.* [2005] have attributed the intrusions to episodic reactivation of this transfer zone, the origin of the magma probably being the Trindade hot spot, which moved eastward with respect to South America during the Late Cretaceous. So, on a regional scale, the lithosphere in SE Brazil may have been susceptible at that time to deformation, as a result of heating and structural inheritance of Brasiliano shear zones.

[45] On a more global scale, two important episodes occurred during the Late Cretaceous. First, the half-spreading rate of the South Atlantic increased to a maximum of ~35 mm/yr at Chron 34 (83 Ma) [*Cande et al.*, 1988; *Nürnberg and Müller*, 1991; *Torsvik et al.*, 2009]. On the other side of the South American plate, at the Pacific margin, the tectonic context changed from extensional to compressional [*Ramos*, 2010], resulting in the development of thrust faults and foreland basins at the edge of the Andes [*Arriagada et al.*, 2006; *Cobbold and Rossello*, 2003]. Moreover, further shortening and subsequent exhumation of

rocks occurred along the orogen [*Jaillard et al.*, 2005; *Jaimes and de Freitas*, 2006; *Martin-Gombojav and Winkler*, 2008; *Tunik et al.*, 2010] during the Peruvian phase of Andean orogeny. *Cobbold et al.* [2007] suggested that the compression was a result of combined ridge-push from both the mid-Atlantic and East-Pacific ridges and that it caused deformation across the continent. Therefore a likely explanation for Late Cretaceous cooling on the southeastern Brazilian margin is deformation and subsequent exhumation of a thermally and/or structurally weakened crust under plate-wide compression.

7.3. Tertiary Evolution

[46] The new data in this paper provide better resolution on the Tertiary history of the onshore margin of SE Brazil than did those in the more regional study of *Cogné et al.* [2011]. During the Palaeogene, most samples remained at more or less constant temperatures, but the NW border of the Taubaté Basin experienced rapid cooling (Figures 9 and 10). *Cogné et al.* [2012] show that the basin formed under transtension during the Palaeocene and Eocene, and this history is coherent with the cooling of the samples. While the basement of the basin was being buried under sediment, the northwest border was subject to erosion. Offshore, In Santos Basin, similar strike-slip faulting of the basement along a Precambrian hinge line was synchronous with
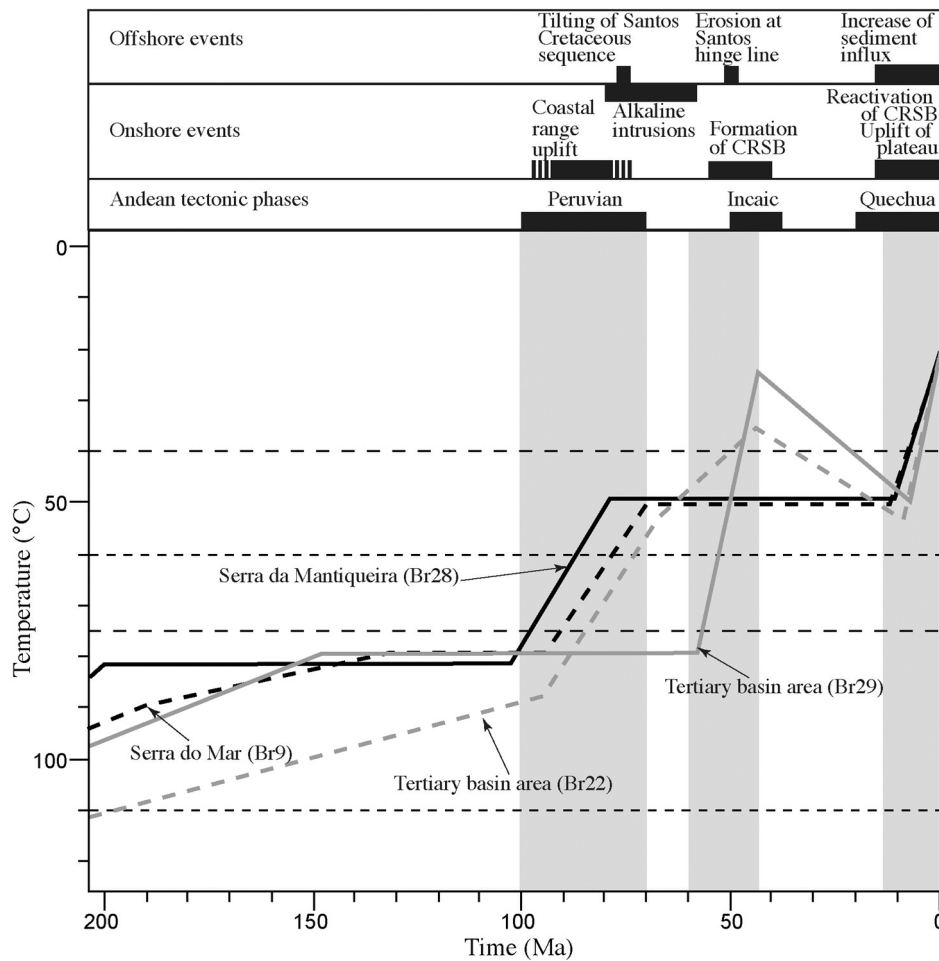
Figure 9. Summary of thermal histories from inverse and forward modeling for whole study area. Grey bars are the same as in Figure 6 and represent episodes of post-breakup cooling. Thin dashed black lines are for PAZ and PRZ (for Durango kinetics). For comparison, we show timing of main events, onshore and offshore SE Brazil, as well as Andean tectonic phases. See text for discussion.

erosion on the shelf of the Santos Basin before deposition of flat-lying mid-Eocene strata [*Cobbold et al.*, 2001].

[47] The timing of this inferred reactivation is synchronous with Eocene exhumation in NE Brazil [*Cobbold et al.*, 2010; *Japsen et al.*, 2012b] and on a plate scale with the Incaic phase of Andean orogeny [*Cobbold et al.*, 2007, and references therein]. Moreover in SE Brazil *Cogné et al.* [2012] argue that the stress field in the Taubaté Basin area was compatible with that in the Andes during the Tertiary. We suggest that the reactivation was due to plate-wide compression and concentrated along Precambrian shear zones, forming the main faults of the Taubaté Basin and the shelf of the offshore Santos Basin.

[48] After this period of deformation, the drainage system changed, as shown through river capture, including the Paraiba do Sul [*Bacoccoli and Aranha*, 1984; *Karner and Driscoll*, 1999]. This led to sediment starvation in the center of the Santos Basin [*Assine et al.*, 2008; *Cobbold et al.*, 2001] and an influx of sediment to the Campos Basin [*Contreras et al.*, 2010; *Mohriak et al.*, 1990, 2008]. However, our thermal history models imply that samples in

the area of the onshore Tertiary basins have undergone reheating from at least the Late Eocene until the Middle Miocene. We suggest that this reheating is the consequence of the burial of the Taubaté Basin borders under about 1 km of lacustrine sedimentary sequence (given the mean geothermal gradient of $25 \pm 5°C$ in the area [*Hamza et al.*, 2005] and the reheating of about 20–30°C) similar to the maximum thickness observed today (Figures 9 and 10). This accumulation could be explained by a drainage that was partly internal. For samples that are now in regions of high elevation (Serras) or on the coast, we cannot exclude the same possibility of burial, but the data are not able to resolve this.

[49] From 15 Ma, the whole area seems to have experienced a final phase of cooling (Figures 9 and 10). This cooling is necessary, to explain the results of forward modeling. However, this is clearly conditional on the assumptions of annealing and diffusion kinetics. At least for fission track annealing, many authors have suggested that a late cooling stage may be a modeling artifact [e.g., *Dempster and Persano*, 2006; *Gunnell*, 2000; *Redfield*, 2010]. However,
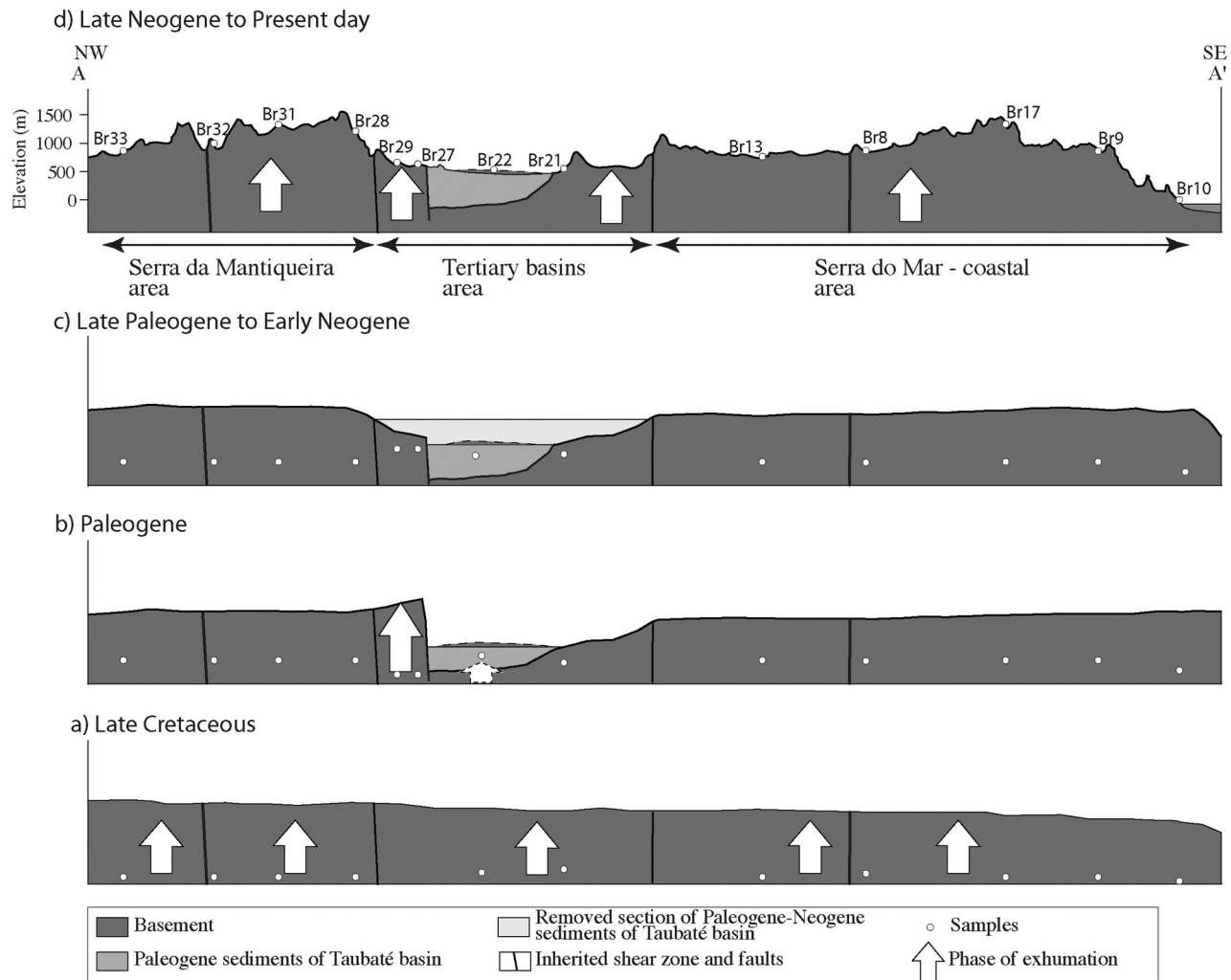
Figure 10. Schematic cross sections showing post-rift evolution of SE Brazilian margin (see Figure 2 for location of profile). (a) During Late Cretaceous, whole area was subject to uplift and erosion and samples cooled. (b) During Early Paleogene, cooling/exhumation occurred only within area of Tertiary basins. (c) During Late Paleogene and Early Neogene, Tertiary basins area is buried under sediments. (d) From Late Neogene until Present-day, entire area underwent uplift and erosion, leading to cooling of samples. See text for discussion.

independent geological information provide support for such late cooling stage in southeast Brazil. The sedimentary influx in the onshore basins is often closely linked to the onshore erosional history [e.g., *Gallagher and Brown*, 1997, 1999; *Modica and Brush*, 2004]. The river Paraiba do Sul, which drained most of the area, had its outlet in the offshore Campos Basin, where the rate of sediment input increased in the Neogene [*Contreras et al.*, 2010; *Mohriak et al.*, 1990, 2008]. Similarly, in the Santos Basin, the rate of sediment input increased at 15 Ma, even if it remained lower than in the Campos Basin [*Assine et al.*, 2008; *Contreras et al.*, 2010]. There is also structural evidence for transpressional reactivation of onshore Tertiary basins [*Cobbold et al.*, 2001; *Cogné et al.*, 2012; *Riccomini et al.*, 2004], as well as of the offshore Campos Basin [*Fetter*, 2009]. Finally, *Modenesi-Gauttieri et al.* [2011] suggest Neogene and Pleistocene uplift to explain their weathering profile in the

Campos do Jordão plateau (in the Serra da Mantiqueira). Uplift of the whole area, with subsequent denudation, explains the enhanced sedimentary influx and the cooling of the samples. Therefore, we infer that Neogene cooling of about 30°C occurred in Southeast Brazil. We note that *Japsen et al.* [2012b] have also inferred a phase of Neogene cooling in NE Brazil.

[50] As the course of the Paraíba do Sul river is parallel to the Além-Paraíba shear zone for more than 200 km, we suggest that, during the uplift of the area, the reactivation of this shear zone led to destruction of the barrier that separated the internal drainage of the Tertiary basins from the external drainage to the Campos Basin. This destruction provoked the formation of a new drainage that was totally external and led to an enhanced erosion and remobilization of the accumulated sediment.

[51] As this phase was synchronous with the Quechua phase of tectonic activity in the Andes, we suggest the reactivation of the whole area may reflect an acceleration of spreading on the East Pacific ridge [*Pardo-Casas and Molnar*, 1987; *Somoza*, 1998], leading to a stronger plate-wide compression, which is still active today. Current seismicity [*Assumpção*, 1998], deformation of Pleistocene or later sediments in the Taubaté Basin [*Riccomini et al.*, 1989] and the World Stress Map (O. Heidbach et al., The World Stress Map database release 2008, doi:10.1594/GFZ.WSM. Rel2008) all provide evidence for ongoing compression in SE Brazil. Moreover, Quaternary uplift driven by compression has resulted in elevated marine terraces around the world and especially in SE Brazil [*Pedoja et al.*, 2011]. We therefore infer that ongoing tectonic denudation and uplift since the Middle Miocene have accounted for rejuvenation of the high relief in southeast Brazil.

8. Conclusions

[52] Having restricted our sampling to an area where there was clear geological evidence of Tertiary tectonic activity, we have been able to exploit thermochronology to better constrain the post breakup history of the onshore margin of SE Brazil, particularly during the Tertiary. Inverse modeling of the thermochronological data implies 3 periods of post-rift accelerated cooling, during (1) the Late Cretaceous, (2) the Palaeogene and (3) the Neogene, and a period of limited reheating. Sensitivity tests using forward modeling enable us to consider different scenarios, consistent with the range of uncertainties associated with the inverse thermal histories. These tests imply that Tertiary reheating is required by the data for the Taubaté area, whereas for current areas of high elevation it is not. The coincidence in timing of cooling in SE Brazil with (1) periods of accelerated cooling in NE Brazil, (2) tectonic events both onshore and offshore and (3) major phases of Andean tectonics, leads us to conclude that the reactivation could be due to plate-wide compressional stress, resulting from the convergence of the Nazca and South American plates. During the Late Cretaceous the crust in SE Brazil may have been sensitive to reactivation, due to structural inheritance (Precambrian shear zones) and/ or thermal weakening (by magmatism and perhaps earlier mantle plume activity). During the Palaeogene, deformation concentrated along the inherited shear zones, leading to localized exhumation at the edges of the Tertiary basins. The same pattern of deformation offshore may have been partly responsible for the current geometry of the Santos Basin, where folds mark the hinge line. The Taubaté Basin area is later buried beneath ∼1 km of sediment. Finally, an increase in the velocity of the convergence between plate led to (1) widespread reactivation of inherited structures, (2) uplift of the area, (3) erosion of the SE Brazilian margin and (4) rejuvenation of the relief during the Neogene. Independent geological information implies that this is not an artifact of inverse modeling. We conclude that the post-breakup evolution of SE Brazil reflects a combination of structural inheritance, magmatic activity and plate-wide stress, leading to post-rift episodic uplift, rather than erosion of rift related uplifted relief. Thus the margin in SE Brazil has not remained passive since the break-up and such concept may be the case for other "passive" margins around the world.

References

Almeida, F. F. M. (1976), The system of continental rifts bordering the Santos Basin, Brazil, *An. Acad. Bras. Cienc.*, *48*, 15–26.

Almeida, F. F. M. (1991), O alinhamento magmatico de Cabo Frio, paper presented at 2nd Simposio de Geologia do Sudeste, Soc. Bras. de Geol., São Paulo, Brazil.

Almeida, F. F. M., and C. D. R. Carneiro (1998), Origem e evolução da Serra do Mar, *Rev. Bras. Geocienc.*, *28*, 135–150.

Arriagada, C., P. R. Cobbold, and P. Roperch (2006), Salar de Atacama basin: A record of compressional tectonics in the central Andes since the mid-Cretaceous, *Tectonics*, *25*, TC1008, doi:10.1029/2004TC001770.

Assine, M. L., F. S. Corrêa, and H. K. Chang (2008), Migração de depocen-tros na Bacia de Santos: Importância na exploração de hidrocarbonetos, *Rev. Bras. Geocienc.*, *38*, 111–127.

Assumpção, M. (1998), Seismicity and stresses in the Brazilian passive margin, *Bull. Seismol. Soc. Am.*, *88*, 160–169.

Bacoccoli, G., and L. G. Aranha (1984), Evolução estrutural fanerozoica do Brasil meridional, internal report, Petrobras, Rio de Janeiro, Brazil.

Barbarand, J., T. Hurford, and A. Carter (2003a), Variation in apatite fission-track length measurement: Implications for thermal history mod-elling, *Chem. Geol.*, *198*, 77–106, doi:10.1016/S0009-2541(02)00423-0.

Barbarand, J., A. Carter, I. Wood, and T. Hurford (2003b), Compositional and structural control of fission-track annealing in apatite, *Chem. Geol.*, *198*, 107–137, doi:10.1016/S0009-2541(02)00424-2.

Braun, J., and P. van der Beek (2004), Evolution of passive margin escarpments: What can we learn from low-temperature thermochronology?, *J. Geophys. Res.*, *109*, F04009, doi:10.1029/2004JF000147.

Brown, R. W., D. J. Rust, M. A. Summerfield, A. J. W. Gleadow, and M. C. J. De Wit (1990), An early Cretaceous phase of accelerated erosion on the south-western margin of Africa: Evidence from apatite fission track analysis and the offshore sedimentary record, *Int. J. Radiat. Appl. Instrum., Part D*, *17*, 339–350, doi:10.1016/1359-0189(90)90056-4.

Brown, R. W., K. Gallagher, A. J. W. Gleadow, and M. A. Summerfield (1999), Morphotectonic evolution of the South Atlantic margins of Africa and South America, in *Geomorphology and Global Tectonics*, edited by M. A. Summerfield, pp. 257–283, John Wiley, Chichester, U. K.

Brown, R. W., M. A. Summerfield, and A. J. W. Gleadow (2002), Denuda-tional history along a transect across the Drakensberg Escarpment of southern Africa derived from apatite fission track thermochronology, *J. Geophys. Res.*, *107*(B12), 2350, doi:10.1029/2001JB000745.

Brown, R., R. Beucher, K. Gallagher, C. Persano, F. M. Stuart, and P. G. Fitzgerald (2011), Exploiting the natural dispersion of single crystal fragment (U-Th)/He age determinations using a new inverse approach to deriving thermal history information, Abstract V31G-06 presented at 2011 Fall Meeting, AGU, San Francisco, Calif., 5–9 Dec.

Cande, S. C., J. L. LaBrecque, and W. F. Haxby (1988), Plate kine-matics of the South Atlantic: Chron C34 to Present, *J. Geophys. Res.*, *93*, 13,479–13,492, doi:10.1029/JB093iB11p13479.

Carlson, W. D., R. A. Donelick, and R. A. Ketcham (1999), Variability of apatite fission-track annealing kinetics: I. Experimental results, *Am. Mineral.*, *84*, 1213–1223.

Chang, H. K., R. O. Kowsmann, A. M. F. Figueiredo, and A. A. Bender (1992), Tectonics and stratigraphy of the East Brazil Rift system: An overview, *Tectonophysics*, *213*, 97–138, doi:10.1016/0040-1951(92)90253-3.

Cherniak, D. J., E. B. Watson, and J. B. Thomas (2009), Diffusion of helium in zircon and apatite, *Chem. Geol.*, *268*, 155–166, doi:10.1016/j.chemgeo.2009.08.011.

Cobbold, P. R., and E. A. Rossello (2003), Aptian to recent compressional deformation, foothills of the Neuquén Basin, Argentina, *Mar. Pet. Geol.*, *20*, 429–443, doi:10.1016/S0264-8172(03)00077-1.

Cobbold, P. R., K. E. Meisling, and V. S. Mount (2001), Reactivation of an obliquely rifted margin, Campos and Santos Basins, southeastern Brazil, *AAPG Bull.*, *85*, 1925–1944.

Cobbold, P. R., E. A. Rossello, P. Roperch, C. Arriagada, L. A. Gómez, and C. Lima (2007), Distribution, timing, and causes of Andean deformation

across South America, in *Deformation of the Continental Crust*, edited by A. C. Ries, R. W. H. Butler, and R. H. Graham, *Geol. Soc. Spec. Publ.*, *272*, 321–343.

Cobbold, P. R., D. Chiossi, P. F. Green, P. Jaspen, and J. Bonow (2010), Compressional reactivation of the Atlantic Margin of Brazil: Structural styles and consequences for hydrocarbon exploration, *Search Discovery*, *2010*, 30114.

Cogné, N., K. Gallagher, and P. R. Cobbold (2011), Post-rift reactivation of the onshore margin of southeast Brazil: Evidence from apatite (U–Th)/He and fission-track data, *Earth Planet. Sci. Lett.*, *309*, 118–130, doi:10.1016/j.epsl.2011.06.025.

Cogné, N., P. R. Cobbold, C. Riccomini, and K. Gallagher (2012), Tectonic setting of the Taubaté Basin (southeastern Brazil): Insights from régional seismic profiles and outcrop data, *J. South Am. Earth Sci.*, in press.

Contreras, J., R. Zühlke, S. Bowman, and T. Bechstädt (2010), Seismic stratigraphy and subsidence analysis of the southern Brazilian margin (Campos, Santos and Pelotas basins), *Mar. Pet. Geol.*, *27*, 1952–1980, doi:10.1016/j.marpetgeo.2010.06.007.

de Brito Neves, B. B., and U. G. Cordani (1991), Tectonic evolution of South America during the Late Proterozoic, *Precambrian Res.*, *53*, 23–40, doi:10.1016/0301-9268(91)90004-T.

Dempster, T. J., and C. Persano (2006), Low-temperature thermochronology: Resolving geotherm shapes or denudation histories?, *Geology*, *34*, 73–76, doi:10.1130/G21980.1.

Donelick, R. A. (1991), Crystallographic orientation dependence of mean etchable fission track length in apatite: An empirical model and experimental observations, *Am. Mineral.*, *76*, 83–91.

Dunkl, I. (2002), Trackkey: A Windows program for calculation and graphical presentation of fission track data, *Comput. Geosci.*, *28*, 3–12, doi:10.1016/S0098-3004(01)00024-3.

Ehlers, T. A., and K. A. Farley (2003), Apatite (U-Th)/He thermochronometry: Methods and applications to problems in tectonic and surface processes, *Earth Planet. Sci. Lett.*, *206*, 1–14, doi:10.1016/S0012-821X(02)01069-5.

Farley, K. A. (2000), Helium diffusion from apatite: General behavior as illustrated by Durango fluorapatite, *J. Geophys. Res.*, *105*, 2903–2914, doi:10.1029/1999JB900348.

Farley, K. A. (2002), (U-Th)/He dating: Techniques, calibrations, and applications, *Rev. Mineral. Geochem.*, *47*, 819–844, doi:10.2138/rmg.2002.47.18.

Farley, K. A., R. A. Wolf, and L. T. Silver (1996), The effects of long alpha-stopping distances on (U-Th)/He ages, *Geochim. Cosmochim. Acta*, *60*, 4223–4229, doi:10.1016/S0016-7037(96)00193-7.

Fetter, M. (2009), The role of basement tectonic reactivation on the structural evolution of Campos Basin, offshore Brazil: Evidence from 3D seismic analysis and section restoration, *Mar. Pet. Geol.*, *26*, 873–886, doi:10.1016/j.marpetgeo.2008.06.005.

Fitzgerald, P. G., S. L. Baldwin, L. E. Webb, and P. B. O'Sullivan (2006), Interpretation of (U-Th)/He single grain ages from slowly cooled crustal terranes: A case study from the Transantarctic Mountains of southern Victoria Land, *Chem. Geol.*, *225*, 91–120, doi:10.1016/j.chemgeo.2005.09.001.

Flowers, R. M., and S. A. Kelley (2011), Interpreting data dispersion and "inverted" dates in apatite (U-Th)/He and fission-track datasets: An example from the US midcontinent, *Geochim. Cosmochim. Acta*, *75*, 5169–5186, doi:10.1016/j.gca.2011.06.016.

Flowers, R. M., R. A. Ketcham, D. L. Shuster, and K. A. Farley (2009), Apatite (U-Th)/He thermochronometry using a radiation damage accumulation and annealing model, *Geochim. Cosmochim. Acta*, *73*, 2347–2365, doi:10.1016/j.gca.2009.01.015.

Galbraith, R. F. (1990), The radial plot: Graphical assessment of spread in ages, *Nucl. Tracks Radiat. Meas.*, *17*, 207–214, doi:10.1016/1359-0189(90)90036-W.

Galbraith, R. F., and G. M. Laslett (1993), Statistical models for mixed fission track ages, *Nucl. Tracks Radiat. Meas.*, *21*, 459–470, doi:10.1016/1359-0189(93)90185-C.

Gallagher, K. (2012), Transdimensional inverse thermal history modeling for quantitative thermochronology, *J. Geophys. Res.*, *117*, B02408, doi:10.1029/2011JB008825.

Gallagher, K., and R. Brown (1997), The onshore record of passive margin evolution, *J. Geol. Soc.*, *154*, 451–457, doi:10.1144/gsjgs.154.3.0451.

Gallagher, K., and R. Brown (1999), The Mesozoic denudation history of the Atlantic margins of southern Africa and southeast Brazil and the relationship to offshore sedimentation, in *The Oil and Gas Habitats of the South Atlantic*, edited by N. R. Cameron, R. H. Bate, and V. S. Clure, *Geol. Soc. Spec. Publ.*, *153*, 41–53.

Gallagher, K., C. J. Hawkesworth, and M. S. M. Mantovani (1994), The denudation history of the onshore continental margin of SE Brazil inferred

from apatite fission track data, *J. Geophys. Res.*, *99*, 18,117–18,145, doi:10.1029/94JB00661.

Gallagher, K., C. J. Hawkesworth, and M. S. M. Mantovani (1995), Denudation, fission track analysis and the long-term evolution of passive margin topography: Application to the southeast Brazilian margin, *J. South Am. Earth Sci.*, *8*, 65–77, doi:10.1016/0895-9811(94)00042-Z.

Gallagher, K., R. Brown, and C. Johnson (1998), Fission track analysis and its applications to geological problems, *Annu. Rev. Earth Planet. Sci.*, *26*, 519–572, doi:10.1146/annurev.earth.26.1.519.

Gautheron, C. E., L. Tassan-Got, and K. A. Farley (2006), (U-Th)/Ne chronometry, *Earth Planet. Sci. Lett.*, *243*, 520–535, doi:10.1016/j.epsl.2006.01.025.

Gautheron, C., L. Tassan-Got, J. Barbarand, and M. Pagel (2009), Effect of alpha-damage annealing on apatite (U-Th)/He thermochronology, *Chem. Geol.*, *266*, 157–170, doi:10.1016/j.chemgeo.2009.06.001.

Gautheron, C., L. Tassan-got, R. A. Ketcham, and K. J. Dobson (2012), Accounting for long alpha-particle stopping distances in (U-Th-Sm)/He geochronology: 3D modeling of diffusion, zoning, implantation, and abrasion, *Geochim. Cosmochim. Acta*, *96*, 44–56.

Gilchrist, A. R., and M. A. Summerfield (1990), Differential denudation and flexural isostasy in formation of rifted-margin upwarps, *Nature*, *346*, 739–742, doi:10.1038/346739a0.

Gilchrist, A. R., and M. A. Summerfield (1994), Tectonic models of passive margin evolution and their implications for theories of long-term landscape development, in *Process Models and Theoretical Geomorphology*, edited by M. J. Kirkby, pp. 55–84, John Wiley, Chichester, U. K.

Gleadow, A. J. W. (1981), Fission-track dating methods: What are the real alternatives?, *Nucl. Tracks*, *5*, 3–14, doi:10.1016/0191-278X(81)90021-4.

Gleadow, A. J. W., I. R. Duddy, P. F. Green, and J. F. Lovering (1986), Confined fission track lengths in apatite: A diagnostic tool for thermal history analysis, *Contrib. Mineral. Petrol.*, *94*, 405–415, doi:10.1007/BF00376334.

Green, P. F. (1986), On the thermo-tectonic evolution of northern England: Evidence from fission track analysis, *Geol. Mag.*, *123*, 493–506, doi:10.1017/S0016756800035081.

Gunnell, Y. (2000), Apatite fission track thermochronology: An overview of its potential and limitations in geomorphology, *Basin Res.*, *12*, 115–132.

Gunnell, Y., and L. Fleitout (2000), Morphotectonic evolution of the Western Ghats, India, in *Geomorphology and Global Tectonics*, edited by M. A. Summerfield, pp. 321–338, John Wiley, Chichester, U. K.

Gunnell, Y., K. Gallagher, A. Carter, M. Widdowson, and A. J. Hurford (2003), Denudation history of the continental margin of western peninsular India since the early Mesozoic: Reconciling apatite fission-track data with geomorphology, *Earth Planet. Sci. Lett.*, *215*, 187–201, doi:10.1016/S0012-821X(03)00380-7.

Hackspacher, P. C. S., A. R. Saad, M. C. S. Ribeiro, D. F. Godoy, and J. C. Hadler Neto (2008), Tectonic reactivation of the South Atlantic Margin, southeastern Brazil, during the Paleogene time: Apatite fission track analysis and U-Th/He systematics, paper presented at 11th International Conference on Thermochronology, Anchorage, Alaska.

Hamza, V. M., R. A. Cardoso, and A. J. L. Gomes (2005), Gradiente e fluxo géotermico na região sudeste: Indícios de calor residual do magmatismo alcalino e implicações para maturação térmica de sedimentos na plataforma continental, paper presented at III Simposio de Vulcanismo e Ambientes Associados, Cabo Frio, Brazil.

Harman, R., K. Gallagher, R. Brown, A. Raza, and L. Bizzi (1998), Accelerated denudation and tectonic/geomorphic reactivation of the cratons of northeastern Brazil during the Late Cretaceous, *J. Geophys. Res.*, *103*, 27,091–27,105, doi:10.1029/98JB02524.

Hiruma, S. T., C. Riccomini, M. C. Modenesi-Gauttieri, P. C. Hackspacher, J. C. H. Neto, and A. O. B. Franco-Magalles (2010), Denudation history of the Bocaina Plateau, Serra do Mar, southeastern Brazil: Relationships to Gondwana breakup and passive margin development, *Gondwana Res.*, *18*, 674–687, doi:10.1016/j.gr.2010.03.001.

Hurford, A. J. (1990), Standardization of fission track dating calibration: Recommendation by the Fission Track Working Group of the I.U.G.S. Subcommission on Geochronology, *Chem. Geol.*, *80*, 171–178.

Hurford, A. J., and P. F. Green (1982), A users' guide to fission track dating calibration, *Earth Planet. Sci. Lett.*, *59*, 343–354, doi:10.1016/0012-821X(82)90136-4.

Hurford, A. J., and P. F. Green (1983), The zeta age calibration of fission-track dating, *Chem. Geol.*, *41*, 285–317, doi:10.1016/S0009-2541(83)80026-6.

Jaillard, E., P. Bengtson, and A. V. Dhondt (2005), Late Cretaceous marine transgressions in Ecuador and northern Peru: A refined stratigraphic framework, *J. South Am. Earth Sci.*, *19*, 307–323, doi:10.1016/j.jsames.2005.01.006.

Jaimes, E., and M. de Freitas (2006), An Albian-Cenomanian unconformity in the northern Andes: Evidence and tectonic significance, *J. South Am. Earth Sci.*, 21, 466–492, doi:10.1016/j.jsames.2006.07.011.

Japsen, P., J. A. Chalmers, P. F. Green, and J. M. Bonow (2012a), Elevated, passive continental margins: Not rift shoulders, but expressions of episodic, post-rift burial and exhumation, *Global Planet. Change*, 90–91, 73–86, doi:10.1016/j.gloplacha.2011.05.004.

Japsen, P., J. Bonow, P. F. Green, P. R. Cobbold, D. Chiossi, R. Lilletveit, L. P. Magnavita, and A. Pedreira (2012b), Episodic burial and exhumation in NE Brazil after opening of the South Atlantic, *Geol. Soc. Am. Bull.*, 124, 800–816, doi:10.1130/B30515.1.

Karner, G., and N. Driscoll (1999), Tectonic and stratigraphic development of the West African and eastern Brazilian Margins: Insights from quantitative basin modeling, in *The Oil and Gas Habitats of the South Atlantic*, edited by N. R. Cameron, R. H. Bate, and V. S. Clure, *Geol. Soc. Spec. Publ.*, 153, 11–40, doi:10.1144/GSL.SP.1999.153.01.02.

Ketcham, R. A., A. Carter, R. A. Donelick, J. Barbarand, and A. J. Hurford (2007), Improved modeling of fission-track annealing in apatite, *Am. Mineral.*, 92, 799–810, doi:10.2138/am.2007.2281.

Leyden, R., W. J. Ludwig, and M. Ewing (1971), Structure of continental margin off Punta del Este, Uruguay, and Rio de Janeiro, Brazil, *AAPG Bull.*, 55, 2161–2173.

Martin-Gombojav, N., and W. Winkler (2008), Recycling of Proterozoic crust in the Andean Amazon foreland of Ecuador: Implications for orogenic development of the northern Andes, *Terra Nova*, 20, 22–31, doi:10.1111/j.1365-3121.2007.00782.x.

Meesters, A. G. C. A., and T. J. Dunai (2002), Solving the production-diffusion equation for finite diffusion domains of various shapes: Part II. Application to cases with [alpha]-ejection and nonhomogeneous distribution of the source, *Chem. Geol.*, 186, 57–73, doi:10.1016/S0009-2541(01)00423-5.

Modenesi-Gauttieri, M. C., M. C. M. de Toledo, S. T. Hiruma, F. Taioli, and H. Shimada (2011), Deep weathering and landscape evolution in a tropical plateau, *Catena*, 85, 221–230, doi:10.1016/j.catena.2011.01.006.

Modica, C. J., and E. R. Brush (2004), Postrift sequence stratigraphy, paleogeography, and fill history of the deep-water Santos Basin, offshore southeast Brazil, *AAPG Bull.*, 88, 923–945, doi:10.1306/01220403043.

Mohriak, W. U., M. S. Melo, J. F. Dewey, and J. R. Maxwell (1990), Petroleum geology of the Campos basin, offshore Brazil, in *Classic Petroleum Provinces*, edited by J. Brooks, *Geol. Soc. Spec. Publ.*, 50, 119–141, doi:10.1144/GSL.SP.1990.050.01.07.

Mohriak, W. U., M. Nemçok, and G. Enciso (2008), South Atlantic divergent margin evolution: Rift-border uplift and salt tectonics in the basins of SE Brazil, in *West Gondwana: Pre-Cenozoic Correlations Across the South Atlantic Region*, edited by R. J. Pankhurst et al., *Geol. Soc. Spec. Publ.*, 294, 365–398.

Nielsen, S. B., et al. (2009), The evolution of western Scandinavian topography: A review of Neogene uplift versus the ICE (isostasy-climate-erosion) hypothesis, *J. Geodyn.*, 47, 72–95, doi:10.1016/j.jog.2008.09.001.

Nürnberg, D., and R. D. Müller (1991), The tectonic evolution of the South Atlantic from Late Jurassic to present, *Tectonophysics*, 191, 27–53, doi:10.1016/0040-1951(91)90231-G.

Osmundsen, P. T., et al. (2010), Fault-controlled alpine topography in Norway, *J. Geol. Soc.*, 167, 83–98, doi:10.1144/0016-76492009-019.

O'Sullivan, P. B., M. M. Mitchell, A. J. O'Sullivan, B. P. Kohn, and A. Gleadow (2000), Thermotectonic history of the Bassian Rise, Australia: Implications for the breakup of eastern Gondwana along Australia's southeastern margins, *Earth Planet. Sci. Lett.*, 182, 31–47, doi:10.1016/S0012-821X(00)00232-6.

Padilha, A. L., N. B. Trivedi, I. Vitorello, and J. M. da Costa (1991), Geophysical constraints on tectonic models of the Taubaté Basin, southeastern Brazil, *Tectonophysics*, 196, 157–172, doi:10.1016/0040-1951(91)90294-3.

Pardo-Casas, F., and P. Molnar (1987), Relative motion of the Nazca (Farallon) and South American Plates since Late Cretaceous time, *Tectonics*, 6, 233–248, doi:10.1029/TC006i003p00233.

Pedersen, V. K., S. B. Nielsen, and K. Gallagher (2012), The post-orogenic evolution of the Northeast Greenland Caledonides constrained from apatite fission track analysis and inverse geodynamic modelling, *Tectonophysics*, 530–531, 318–330, doi:10.1016/j.tecto.2012.01.018.

Pedoja, K., et al. (2011), Relative sea-level fall since the last interglacial stage: Are coasts uplifting worldwide?, *Earth Sci. Rev.*, 108, 1–15, doi:10.1016/j.earscirev.2011.05.002.

Pereira, M. J., and J. M. Macedo (1990), A Bacia de Santos: Perspectivas de uma nova provincia petrolífera na plataforma continental sudeste brasileira, *Bol. Geocienc. Petrobras*, 4, 3–11.

Persano, C., P. Bishop, and F. M. Stuart (2006), Apatite (U–Th)/He age constraints on the Mesozoic and Cenozoic evolution of the Bathurst region, New South Wales: Evidence for antiquity of the continental drainage divide along a passive margin, *Aust. J. Earth Sci.*, 53, 1041–1050, doi:10.1080/08120090600923303.

Raab, M. J., R. W. Brown, K. Gallagher, A. Carter, and K. Weber (2002), Late Cretaceous reactivation of major crustal shear zones in northern Namibia: Constraints from apatite fission track analysis, *Tectonophysics*, 349, 75–92, doi:10.1016/S0040-1951(02)00047-1.

Ramos, V. A. (2010), The tectonic regime along the Andes: Present-day and Mesozoic regimes, *Geol. J.*, 45, 2–25, doi:10.1002/gj.1193.

Redfield, T. F. (2010), On apatite fission track dating and the Tertiary evolution of West Greenland topography, *J. Geol. Soc.*, 167, 261–271, doi:10.1144/0016-76492009-036.

Reiners, P. W., and K. A. Farley (2001), Influence of crystal size on apatite (U-Th)/He thermochronology: An example from the Bighorn Mountains, Wyoming, *Earth Planet. Sci. Lett.*, 188, 413–420, doi:10.1016/S0012-821X(01)00341-7.

Ribeiro, M. C. S. (2007), Termocronologia e história denudacional da Serra do Mar e implicações no controle deposicional da Bacia de Santos, 211 pp., Inst. of Geosci. and Earth Sci., Univ. of São Paulo, São Paulo, Brazil.

Riccomini, C., A. U. G. Peloggia, J. C. L. Saloni, M. W. Kohnke, and R. M. Figueira (1989), Neotectonic activity in the Serra do Mar rift system (southeastern Brazil), *J. South Am. Earth Sci.*, 2, 191–197, doi:10.1016/0895-9811(89)90046-1.

Riccomini, C., L. G. Sant'Anna, and A. L. Ferrari (2004), Evolução geológica do Rift Continental do Sudeste do Brasil, in *Geologia do Continente Sul-Americano: Evolução da Obra de Fernando Flávio Marques de Almeida*, edited by V. Mantesso Neto et al., pp. 383–405, Edições Beca, São Paulo, Brazil.

Riccomini, C., V. F. Velázquez, and C. B. Gomes (2005), Tectonic controls of the Mesozoic and Cenozoic alkaline magmatism in central-southeastern Brazilian Platform, in *Mesozoic to Cenozoic Alkaline Magmatism in the Brazilian Platform*, edited by C. B. Gomes and P. Comin-Chiaramonti, pp. 31–55, EDUSP-FAPESP, São Paulo, Brazil.

Sant'Anna, L. G., C. Riccomini, B. H. Rodrigues-Francisco, A. N. Sial, M. D. Carvalho, and C. A. V. Moura (2004), The Paleocene travertine system of the Itaboraí basin, southeastern Brazil, *J. South Am. Earth Sci.*, 18, 11–25, doi:10.1016/j.jsames.2004.08.005.

Shuster, D. L., and K. A. Farley (2009), The influence of artificial radiation damage and thermal annealing on helium diffusion kinetics in apatite, *Geochim. Cosmochim. Acta*, 73, 183–196, doi:10.1016/j.gca.2008.10.013.

Shuster, D. L., R. M. Flowers, and K. A. Farley (2006), The influence of natural radiation damage on helium diffusion kinetics in apatite, *Earth Planet. Sci. Lett.*, 249, 148–161, doi:10.1016/j.epsl.2006.07.028.

Somoza, R. (1998), Updated Nazca (Farallon)–South America relative motions during the last 40 My: Implications for mountain building in the central Andean region, *J. South Am. Earth Sci.*, 11, 211–215, doi:10.1016/S0895-9811(98)00012-1.

Tello Saenz, C. A., P. C. Hackspacher, J. C. Hadler Neto, P. J. Iunes, S. Guedes, L. F. B. Ribeiro, and S. R. Paulo (2003), Recognition of Cretaceous, Paleocene, and Neogene tectonic reactivation through apatite fission-track analysis in Precambrian areas of southeast Brazil: Association with the opening of the south Atlantic Ocean, *J. South Am. Earth Sci.*, 15, 765–774, doi:10.1016/S0895-9811(02)00131-1.

Tello Saenz, C. A., J. C. Hadler Neto, P. J. Iunes, S. Guedes, P. C. Hackspacher, L. F. B. Ribeiro, S. R. Paulo, and A. M. Osorio A (2005), Thermochronology of the South American platform in the state of São Paulo, Brazil, through apatite fission tracks, *Radiat. Meas.*, 39, 635–640, doi:10.1016/j.radmeas.2004.08.005.

Torsvik, T. H., S. Rousse, C. Labails, and M. A. Smethurst (2009), A new scheme for the opening of the South Atlantic Ocean and the dissection of an Aptian salt basin, *Geophys. J. Int.*, 177, 1315–1333, doi:10.1111/j.1365-246X.2009.04137.x.

Trouw, R., M. Heilbron, A. Ribeiro, F. Paciullo, C. M. Valeriano, J. C. H. Almeida, M. Tupinamba, and R. R. Andreis (2000), The central segment of the Ribeira Belt, in *Tectonic Evolution of South America*, edited by U. G. Cordani et al., pp. 355–365, Fundo Setorial de Pet. e Gás Nat., Rio de Janeiro, Brazil.

Tunik, M., A. Folguera, M. Naipauer, M. Pimentel, and V. A. Ramos (2010), Early uplift and orogenic deformation in the Neuquén Basin: Constraints on the Andean uplift from U-Pb and Hf isotopic data of detrital zircons, *Tectonophysics*, 489, 258–273, doi:10.1016/j.tecto.2010.04.017.

van der Beek, P., P. Andriessen, and S. Cloetingh (1995), Morphotectonic evolution of rifted continental margins: Inferences from a coupled tectonic-surface processes model and fission track thermochronology, *Tectonics*, 14, 406–421, doi:10.1029/94TC02445.

Warnock, A. C., P. K. Zeitler, R. A. Wolf, and S. C. Bergman (1997), An evaluation of low-temperature apatite U-Th/He thermochronometry,

Geochim. Cosmochim. Acta, *61*, 5371–5377, doi:10.1016/S0016-7037(97)00302-5.

Wolf, R. A., K. A. Farley, and L. T. Silver (1996), Helium diffusion and low-temperature thermochronometry of apatite, *Geochim. Cosmochim. Acta*, *60*, 4231–4240, doi:10.1016/S0016-7037(96)00192-5.

Wolf, R. A., K. A. Farley, and D. M. Kass (1998), Modeling of the temperature sensitivity of the apatite (U-Th)/He thermochronometer, *Chem. Geol.*, *148*, 105–114, doi:10.1016/S0009-2541(98)00024-2.

Zalan, P. V., and J. A. B. de Oliveira (2005), Origem e evolução estrutural do sistema de riftes Cenozóicos do Sudeste do Brasil, *Bol. Geocienc. Petrobras*, *13*, 269–300.